SUPPORTING INFORMATION

Unraveling the Binding, Proton Blockage and Inhibition of the influenza M2 WT and S31N by Rimantadine variants

Antonios Drakopoulos,[1] Christina Tzitzoglaki,[1] Kelly McGuire,[2] Anja Hoffmann,[3] Athina Konstantinidi,[1] Dimitrios Kolocouris,[1] Chunlong Ma,[4] Kathrin Freudenberger,[5] Johanna Hutterer,[5] Günter Gauglitz,[5] Jun Wang,[4] Michaela Schmidtke,[3] David D. Busath,[2] Antonios Kolocouris[1,*]

[1] Department of Pharmaceutical Chemistry, Faculty of Pharmacy, National and Kapodistrian University of Athens, Greece
[2] Dept. of Physiology and Developmental Biology, Brigham Young University, Provo, UT 84602
[3] Jena University Hospital, Department of Medicinal Microbiology, Section Experimental Virology, Hans Knoell Str. 2, D-07745 Jena, Germany
[4] Department of Pharmacology and Toxicology, College of Pharmacy, University of Arizona, Tucson, AZ 85721, USA
[5] Institut für Physikalische und Theoretische Chemie, Eberhard-Karls-Universität Tübingen, Germany

2/14/2018

[*]Addresses: (A.K.) Panepistimioupolis – Zografou, Athens 15771, Greece; Phone: (+301) 210-7274834, Fax: (+301) 210 727 4747; E-Mail: ankol@pharm.uoa.gr

Table of Contents

Peptide synthesis

M2TM peptides corresponding to residues 22-46 of Udorn/72 wild type sequence of M2 (C-terminally amidated $M2TM_{Udorn/72}$: SSDPLVVAASIIGILHLILWILDRL) were synthesized by standard Fmoc solid phase peptide synthesis using an aminomethyl polystyrene resin loaded with the amide linker and purified by reverse phase HPLC. A purification procedure previously described [1] and modified was used. [2] The final peptide purity was 98%.

Compound synthesis

For the synthesis of primary *tert*-alkyl amines **3-5** the raw *tert*-alkyl alcohols **7a-c** were prepared according to Scheme 2 of the manuscript from the reaction between 1-adamantane carbonyl chloride **6** and an organometallic reagent. *Tert*-alkyl alcohol **7a** was prepared in high yield from the reaction between 1-adamantane carbonyl chloride **6** and methylmagnesium iodide. *Tert*-alkyl alcohol **7b** was prepared in high yield from the reaction between 1-adamantane carbonyl chloride **6** and ethyl lithium. The reaction of allylmagnesium bromide with 1-adamantane carbonyl chloride **6** afforded diallyl alcohol **8** which was subsequently hydrogenated under PtO_2 as the catalyst to afford *tert*-alkyl alcohol **7c**. Treatment of *tert*-alkyl alcohols **7a,b** with NaN_3/TFA in dichloromethane afforded azides **9a,b** in high yields. Azides **9a,b** were subjected to reduction through $LiAlH_4$ to form *tert*-alkyl amine **3** in a good yield and **4** in a moderate yield. The same procedure when applied for the synthesis of amine **5** afforded azide **9c** with 37% yield but the yield for the reduction step was 14% due to the formation of unsaturated products and extensive decomposition.

The procedure leading to the synthesis of **3** was described in the Supporting Information of ref. **Error! Bookmark not defined.** of the draft.

3-(Tricyclo[3.3.1.1$^{3.7}$]dec-1-yl)-pentan-3-ol (AdEt$_2$C-OH) 7b. A solution of 1-adamantanecarbonyl chloride **6** (700 mg, 3.53 mmol) in 25 mL of dry diethyl ether was added dropwise under Ar atmosphere and stirring, to a solution of 5 mL ethyl lithium (0.5 M in benzene/cyclohexane, 12.5 mmol). The mixture was stirred for 26 h under Ar atmosphere at room temperature. The reaction mixture was hydrolyzed with an equal volume of saturated ammonium chloride solution under ice-cooling. The organic layer was separated and the aqueous phase was extracted with diethyl ether two times. The combined organic phase was washed two times with a solution of sodium hydroxide 3% w/v, water and brine, and dried over anhydrous sodium sulfate. After evaporation of the solvent under vacuum, a light yellow coloured solid residue of the alcohol **7b** was obtained. Yield 357mg (45.5%); IR (Nujol): ν(OH) 3502 cm^{-1} (br s); ^{1}H-NMR (400MHz, $CDCl_3$) δ: 0.93 (t, J~7 Hz, 6H, 2xCH_3), 1.56 (q, J~7 Hz, 4H, 2x$CH_3\underline{CH_2}$), 1.61-1.70 (m, 12H, 2,4,6,8,9,10-H, adamantane H), 2.05 (br s, 3H, 3,5,7-H, adamantane H); ^{13}C-NMR (200MHz, $CDCl_3$) δ: 9.47 (CH_3), 25.93 ($CH_3\underline{C}H_2$), 28.90 (3,5,7-C, adamantane C), 36.71 (2,8,9-C, adamantane C), 37.40 (4,6,10-C, adamantane C), 38.51 (1-C, adamantane C), 40.48 (C-OH). $C_{15}H_{26}O$, HRMS Calcd: 222.198365, Found: 222.099854

3-(Tricyclo[3.3.1.1$^{3.7}$]dec-1-yl)-pentan-3-amine (AdEt$_2$C-NH$_2$) 4. The oily 3-(1-adamantyl)-3-azido-pentane **8b** was prepared by treatment of the tertiary alcohol **7b** with CH_2Cl_2/NaN_3/TFA according to the same procedure followed for 2-(1-adamantyl)-2-azido-propane **9a**. The reaction afforded an oily mixture of azide **9b** along with 3-(1-adamantyl)-pent-2-ene as an elimination by-product. The yield of the azide preparation was 65 % based on the integration of ^{13}C NMR peaks. The crude oily mixture was used without further purification for the $LiAlH_4$ reduction step.

3-(1-Adamantyl)-3-pentanamine **4** was prepared through $LiAlH_4$ reduction of azide **9b** in refluxing ether for 5h according to the same procedure followed for 2-(1-adamantyl)-propan-2-amine **3**. Amine **4** was afforded as a light yellow colored oil. Yield: 11%; LRMS: 222.4; ^{1}H-NMR (400 MHz, $CDCl_3$) δ: 0.88 (t, J~7 Hz, 6H, 2xCH_3), 1.08 (br s, 2H, NH_2), 1.33-1.52 (m, 2H, 2x$CH_3\underline{CH_2}$), 1.60-1.69 (m, 12H, 2,4,6,8,9,10-H, adamantane H), 1.97 (br s, 3H, 3,5,7-H, adamantane H); ^{13}C-NMR (200MHz, $CDCl_3$) δ: 9.90 (CH_3), 26.73 ($CH_3\underline{C}H_2$), 29.04 (3,5,7-C, adamantane C), 36.75 (2,8,9-C, adamantane C), 37.45 (4,6,10-C, adamantane C), 38.60 (1-C, adamantane C), 39.86 (C-NH_2). Anal. Fumarate ($C_{19}H_{31}NO_4$) (EtOH-Ether) HRMS Calcd: 337.225309, Found: 337.276298

4-(Tricyclo[3.3.1.1$^{3.7}$]dec-1-yl)-hept-1,6-dien-4-ol (AdAllyl$_2$C-OH) 8. Allylmagnesium bromide was prepared from magnesium turnings (1.33 g, 55.4 mmol) and allyl bromide (6.1 g, 50.4 mmol) in 60 mL of dry diethyl ether. A solution of 1-adamantanecarbonyl chloride **6** (2 g, 10.1 mmol) in 60 mL of dry diethyl ether was added dropwise to the first solution, under Ar atmosphere and stirring. The reaction mixture was heated at gentle reflux for 4h under stirring and Ar atmosphere and an additional 24 h at room temperature under stirring and Ar atmosphere.

The mixture was hydrolyzed with an equal volume of saturated solution of ammonium chloride under ice-cooling. The organic layer was separated and the aqueous phase was extracted with diethyl ether two times. The combined organic phase was washed with water and brine, dried (Na_2SO_4) and evaporated under vacuum to yield a yellow colored oil residue of 4-(adamant-1-yl)-hept-1,6-dien-4-ol **8**. Yield: 1.74 g (70%); IR (Film) δ: ν(OH) 3568 cm^{-1} (s), ν(=C-H) 3074 cm^{-1} (s), 3008 cm^{-1} (m), ν(C=C) 1636 cm^{-1} (s); ^{1}H-NMR (400MHz, $CDCl_3$) δ: 1.70 (m, 12H, 2,4,6,8,9,10-H, adamantane H), 1.99 (br s, 3H, 3,5,7-H, adamantane H), 2.28-2.40 (m, *J*~7 Hz, 4H, 3,5-CH_2), 5.09 (t, *J*~7 Hz, 4H, 2xCH_2=), 5.88-5.98 (m, *J*~7 Hz, 2H, 2xCH=); ^{13}C-NMR (200MHz, $CDCl_3$) δ: 28.81 (3,5,7-C, adamantane C), 36.57 (2,8,9-C, adamantane C), 37.29 (4,6,10-C, adamantane C), 39.29 (CH_2), 40.34 (1-C, adamantane C), 76.08 (C-OH), 118.11 (=CH_2), 135.82 (CH=). $C_{17}H_{26}O$ HRMS Calcd: 246.198365, Found: 246.159789

4-(Tricyclo[3.3.1.1$^{3.7}$]dec-1-yl)-heptan-4-ol (AdPr$_2$C-OH) 7c. The 4-(adamant-1-yl)-hept-1,6-dien-4-ol **8** (840 mg, 3.42 mmol) was dissolved in 80 mL of absolute ethanol and the solution was hydrogenated over Adams catalyst (80 mg) for 20 h. Vacuum filtration of the catalyst and solvent evaporation under vacuum yields a white solid residue of 4-(1-adamant-1-yl)-heptan-4-ol **7c**. Yield: 720 mg (84%); IR (Nujol): ν(OH) 3469 cm^{-1} (s), ^{1}H-NMR (400MHz, $CDCl_3$) δ: 0.90 (t, *J*~7 Hz, 6H, 1, 2xCH_3), 1.29-1.39 (m, *J*~7 Hz, 4H, 2,6-CH_2), 1.41-1.50 (m, *J*~7 Hz, 4H, 3,5-CH_2), 1.65 (m, 12H, 2,4,6,8,9,10-H, adamantane H), 1.98 (br s, 3H, 3,5,7-H, adamantane H), 2.17 (s, 1H, -OH); ^{13}C-NMR (200MHz, $CDCl_3$) δ: 15.29 (CH_3), 18.19 (CH_2), 28.89 (3,5,7-C, adamantane C), 36.59 (2,8,9-C, adamantane C), 36.88 (CH_2), 37.39 (4,6,10-C, adamantane C), 40.28 (1-C, adamantane C), 41.39 (C-OH). $C_{17}H_{30}O$ HRMS Calcd: 250.229665, Found: 250.129573

4-(Tricyclo[3.3.1.1$^{3.7}$]dec-1-yl)-heptan-4-amine (AdPr$_2$C-NH$_2$) 5. The oily 3-(adamant-1-yl)-heptan-4-azide **9c** was prepared by treatment of the tertiary alcohol **7c** with CH_2Cl_2/NaN_3/TFA as previously described. The reaction afforded a yellow colored oily mixture consisting of the desired 3-(adamant-1-yl)-4-azido-heptane **9c** (54 %) and of 4-(adamant-1-yl)-hept-3-ene (46%) as an elimination byproduct. Yield of the azide: 37%. The crude oily mixture was used without further purification for the $LiAlH_4$ reduction step. 4-(Adamant-1-yl)-heptan-4-amine **5** was prepared through $LiAlH_4$ reduction of azide **9c** in refluxing ether for 5h according to the same procedure described previously. Amine **5** was afforded as a light yellow coloured oil. Yield (based on azide): 14%; MS: 250.1; ^{1}H-NMR (400MHz, $CDCl_3$) δ: 0.89 (t, *J*~7 Hz, 6H, 2xCH_3), 1.19 (br s, 2H, NH_2), 1.25-1.41 (m, *J*~7 Hz, 8H, 4xCH_2), 1.61 (m, 12H, 2,4,6,8,9,10-H, adamantane H), 1.98 (br s, 3H, 3,5,7-H, adamantane H); ^{13}C-NMR (200MHz, $CDCl_3$) δ: 15.45 (CH_3), 18.59 (CH_2), 29.07 (3,5,7-C, adamantane C), 36.65 (2,8,9-C, adamantane C), 37.45 (CH_2), 37.97 (4,6,10-C, adamantane C), 39.53 (1-C, adamantane C), 56.94 (C-N). Anal. Fumarate ($C_{21}H_{35}NO_4$) (EtOH-Ether) HRMS Calcd: 365.256609, Found: 365.113981

^{1}H NMR Spectra

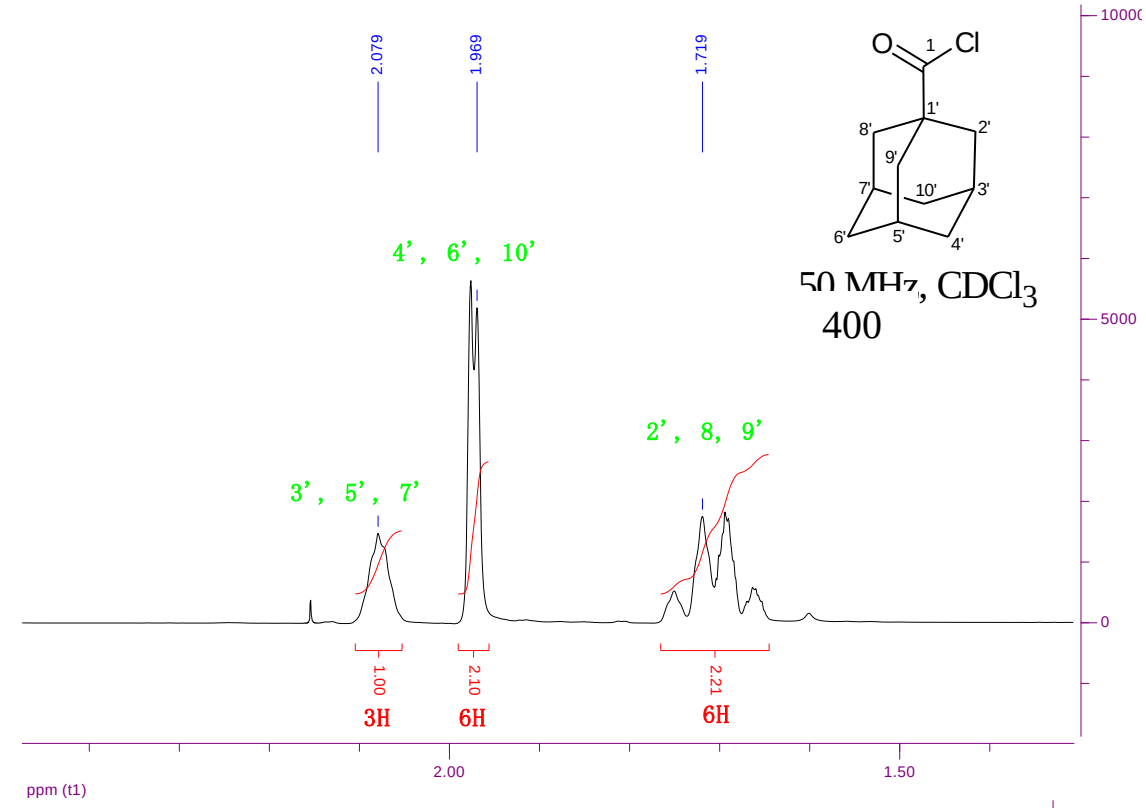
2.079
1.969
1.719
O
1
Cl
1'
2'
3'
4'
5'
6'
7'
8'
9'
10'
4', 6', 10'
50 MHz, CDCl3
400
2', 8, 9'
3', 5', 7'
1.00
2.10
2.21
3H
6H
6H
10000
5000
0
2.00
1.50
ppm (t1)

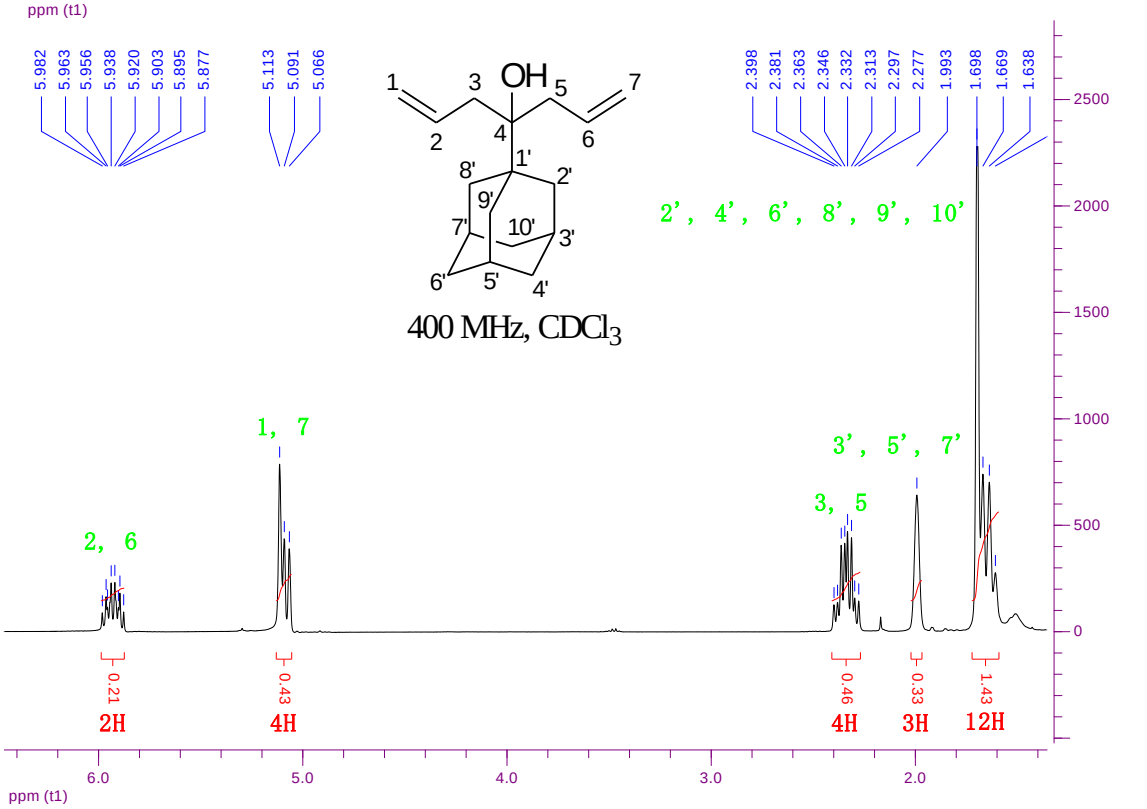
5.982
5.963
5.956
5.938
5.920
5.903
5.895
5.877
5.113
5.091
5.066
2.398
2.381
2.363
2.346
2.332
2.313
2.297
2.277
1.993
1.698
1.669
1.638
OH
1
2
3
4
5
6
7
1'
2'
3'
4'
5'
6'
7'
8'
9'
10'
400 MHz, CDCl3
2', 4', 6', 8', 9', 10'
1, 7
2, 6
3', 5', 7'
3, 5
0.21
0.43
0.46
0.33
1.43
2H
4H
4H
3H
12H
2500
2000
1500
1000
500
0
6.0
5.0
4.0
3.0
2.0
ppm (t1)

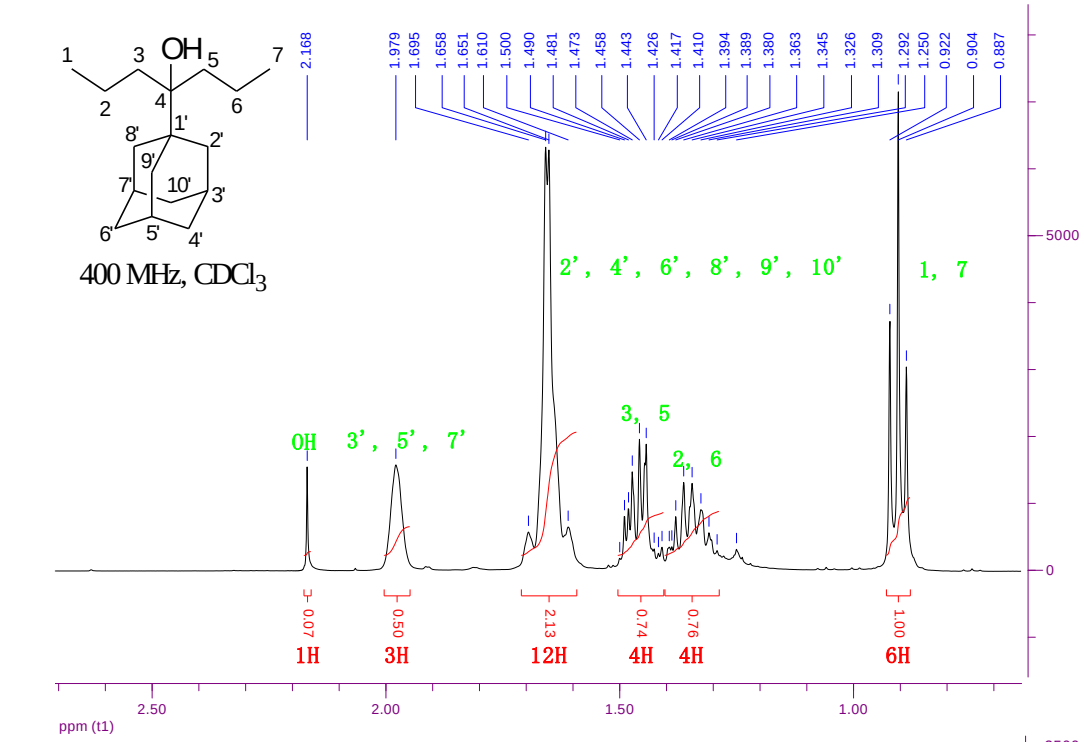
400 MHz, CDCl3
2.168
1.979
1.695
1.658
1.651
1.610
1.500
1.490
1.481
1.473
1.458
1.443
1.426
1.417
1.410
1.394
1.389
1.380
1.363
1.345
1.326
1.309
1.292
1.250
0.922
0.904
0.887
2', 4', 6', 8', 9', 10'
1, 7
OH
3', 5', 7'
3, 5
2, 6
0.07
0.50
2.13
0.74
0.76
1.00
1H
3H
12H
4H
4H
6H
5000
0
2.50
2.00
1.50
1.00
ppm (t1)

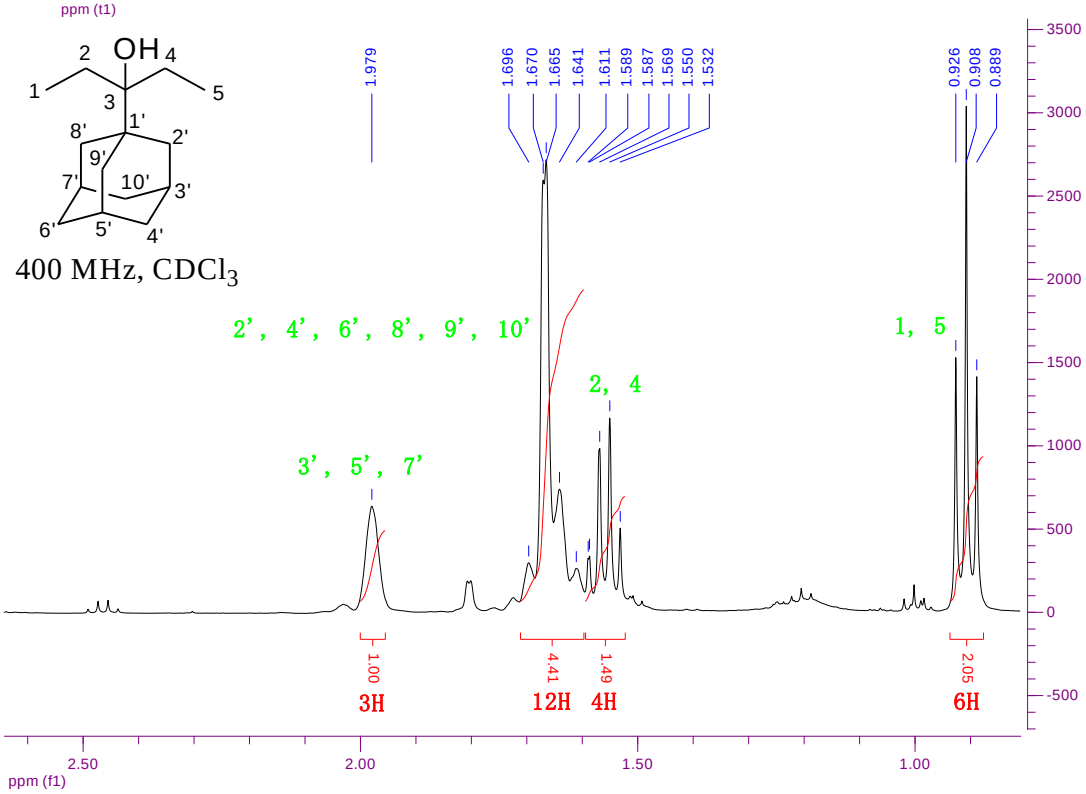
400 MHz, CDCl3
1.979
1.696
1.670
1.665
1.641
1.611
1.589
1.587
1.569
1.550
1.532
0.926
0.908
0.889
2', 4', 6', 8', 9', 10'
1, 5
2, 4
3', 5', 7'
1.00
4.41
1.49
2.05
3H
12H
4H
6H
3500
3000
2500
2000
1500
1000
500
0
-500
2.50
2.00
1.50
1.00
ppm (f1)

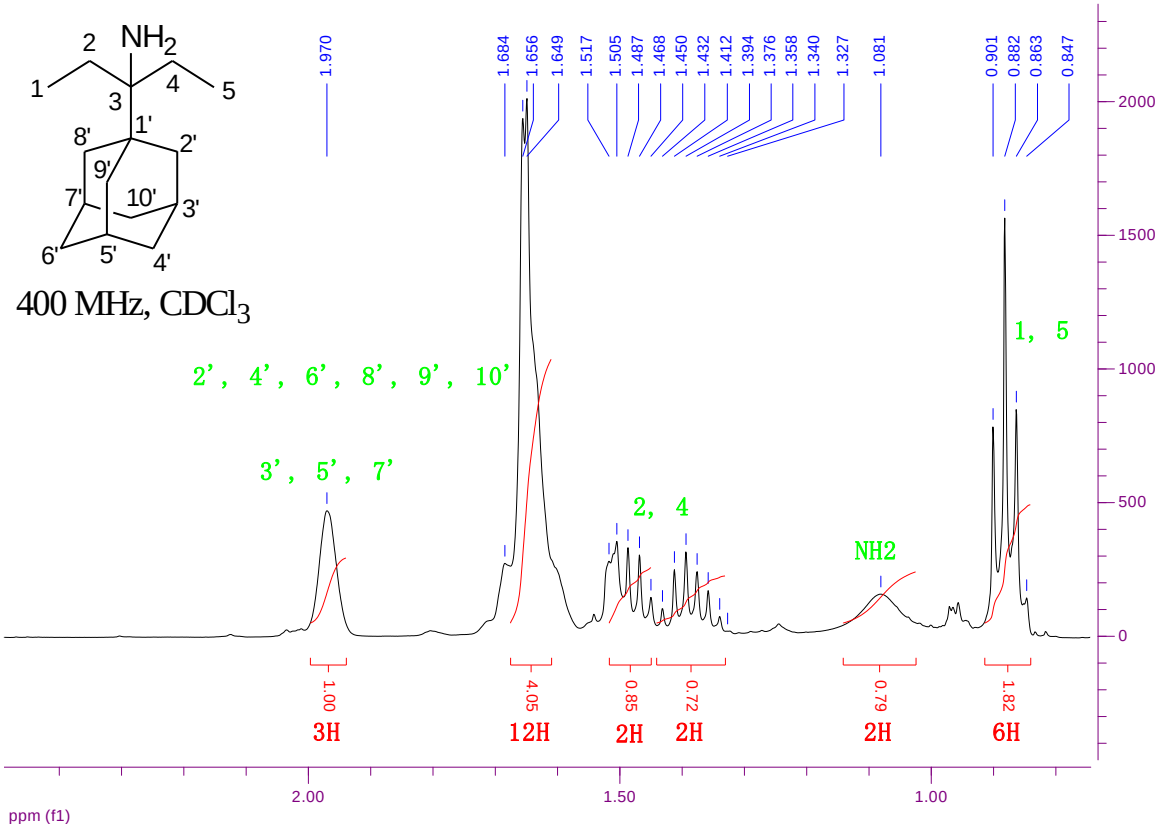
NH2
400 MHz, CDCl3
1.970
1.684
1.656
1.649
1.517
1.505
1.487
1.468
1.450
1.432
1.412
1.394
1.376
1.358
1.340
1.327
1.081
0.901
0.882
0.863
0.847
2', 4', 6', 8', 9', 10'
3', 5', 7'
2, 4
NH2
1, 5
1.00
4.05
0.85
0.72
0.79
1.82
3H
12H
2H
2H
2H
6H
2000
1500
1000
500
0
2.00
1.50
1.00
ppm (f1)

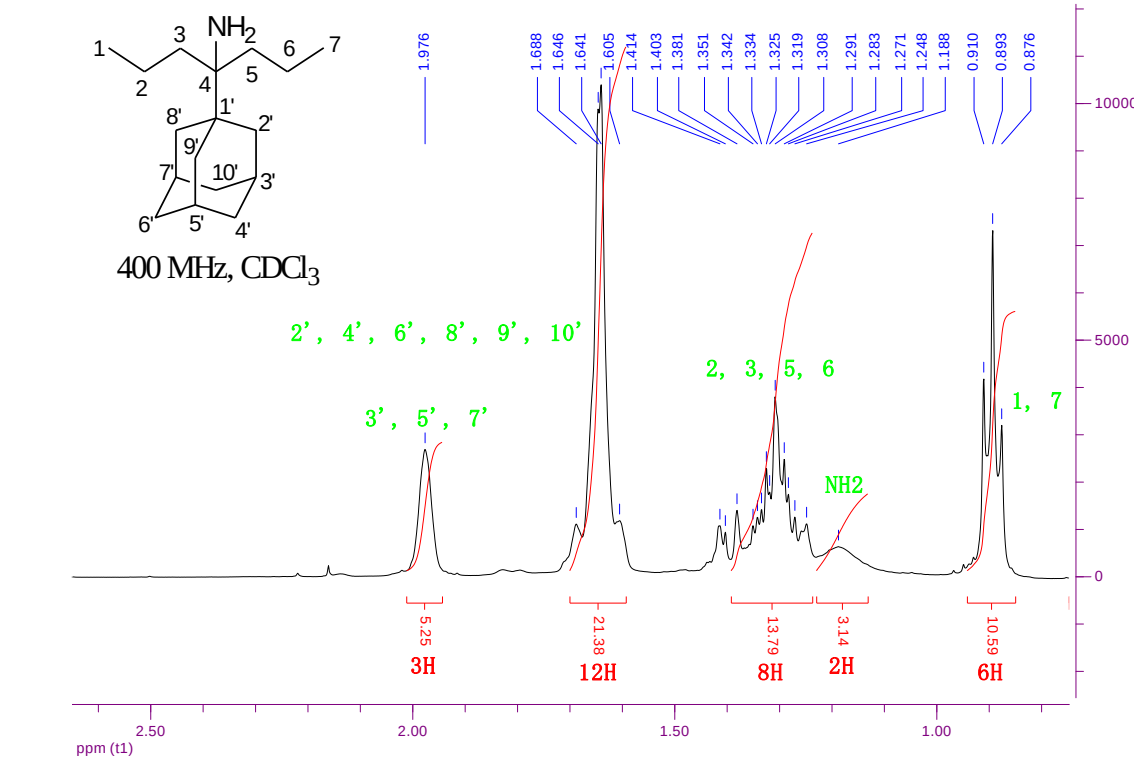
NH2
400 MHz, CDCl3
1.976
1.688
1.646
1.641
1.605
1.414
1.403
1.381
1.351
1.342
1.334
1.325
1.319
1.308
1.291
1.283
1.271
1.248
1.188
0.910
0.893
0.876
2', 4', 6', 8', 9', 10'
3', 5', 7'
2, 3, 5, 6
NH2
1, 7
5.25
21.38
13.79
3.14
10.59
3H
12H
8H
2H
6H
10000
5000
0
2.50
2.00
1.50
1.00
ppm (t1)

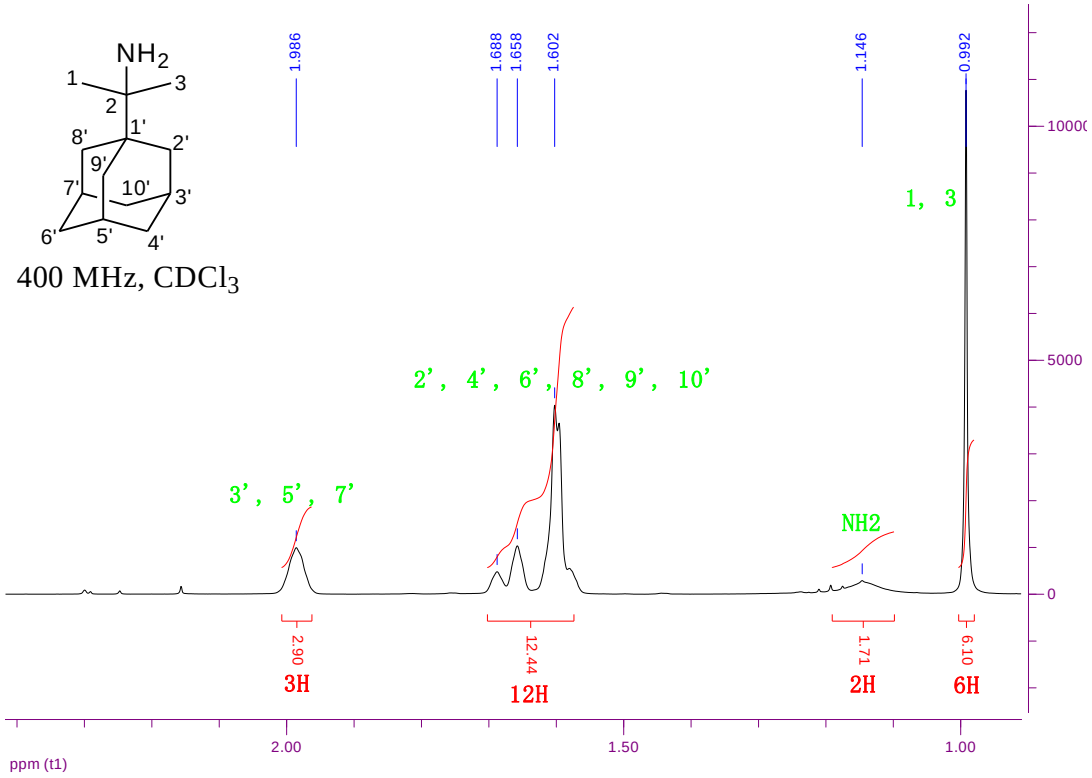
NH2
1
2
3
1'
2'
3'
4'
5'
6'
7'
8'
9'
10'
400 MHz, CDCl3
1.986
1.688
1.658
1.602
1.146
0.992
1, 3
2', 4', 6', 8', 9', 10'
3', 5', 7'
NH2
2.90
12.44
1.71
6.10
3H
12H
2H
6H
2.00
1.50
1.00
ppm (t1)
10000
5000
0

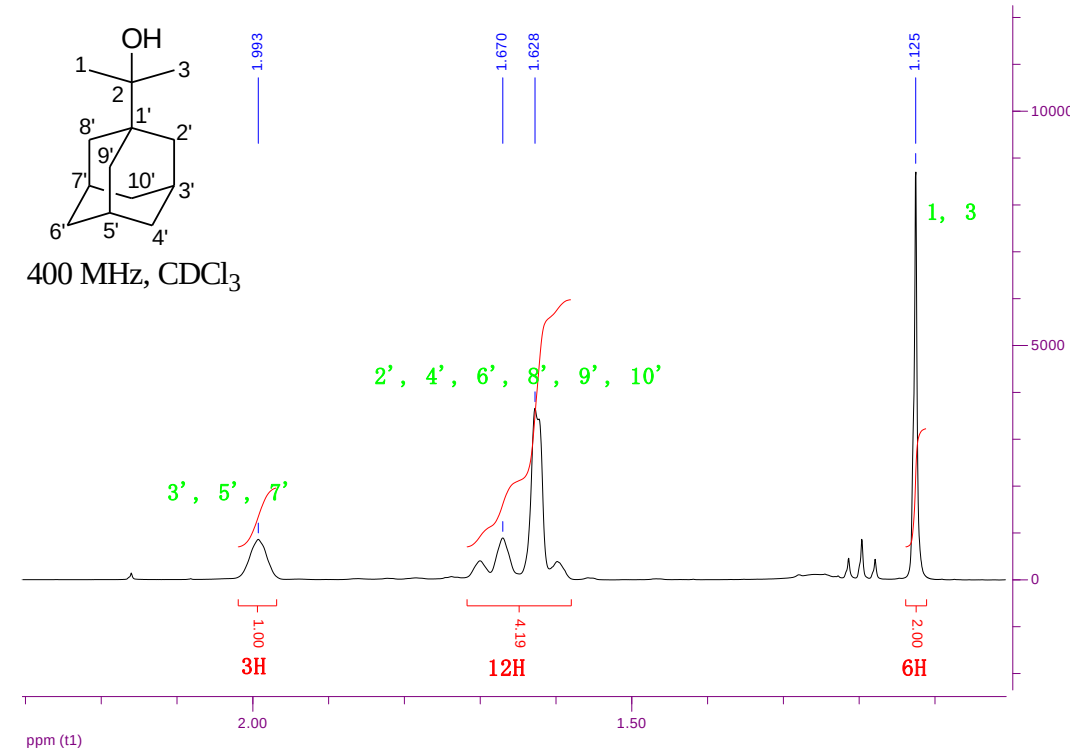
OH
1
2
3
1'
2'
3'
4'
5'
6'
7'
8'
9'
10'
400 MHz, CDCl3
1.993
1.670
1.628
1.125
1, 3
2', 4', 6', 8', 9', 10'
3', 5', 7'
1.00
4.19
2.00
3H
12H
6H
2.00
1.50
ppm (t1)
10000
5000
0

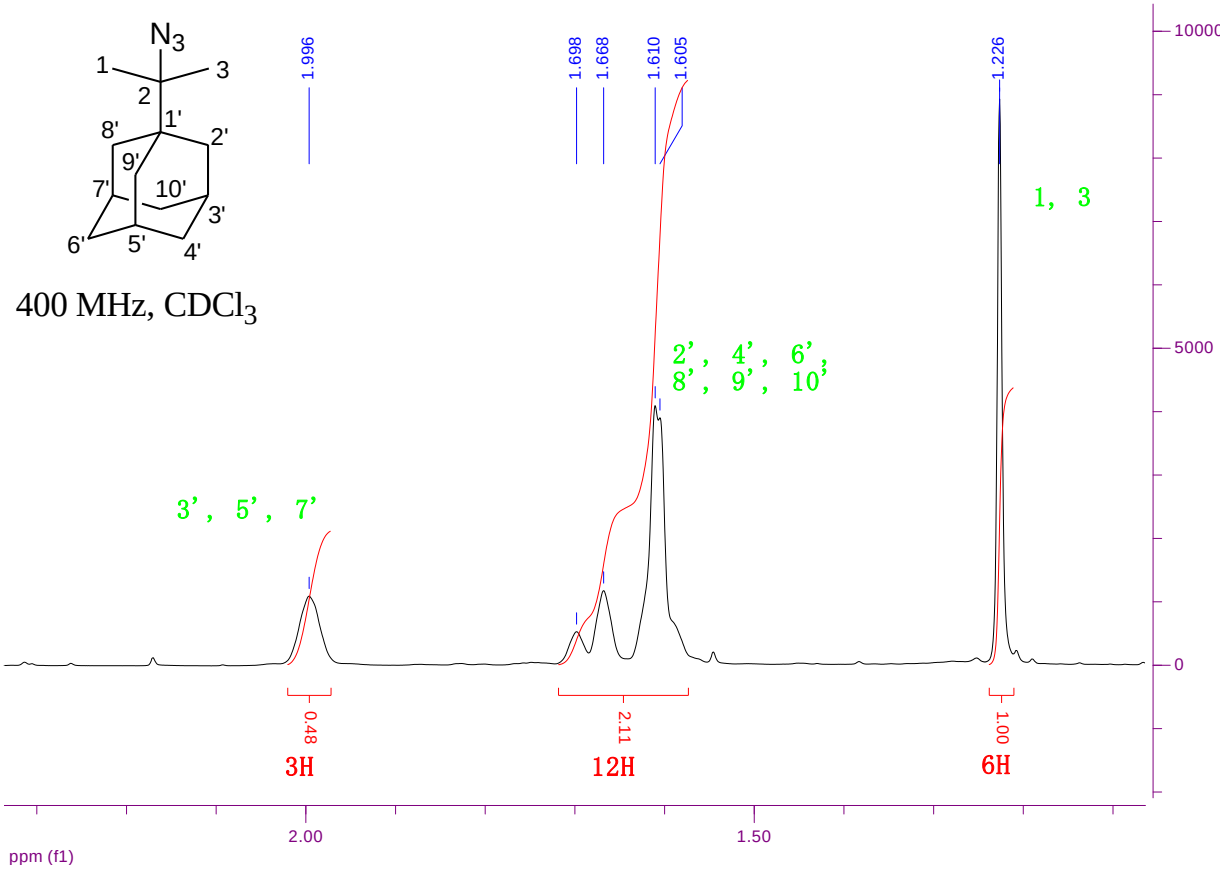
N3
1
2
3
1'
2'
8'
9'
7'
10'
3'
6'
5'
4'
400 MHz, CDCl3
1.996
1.698
1.668
1.610
1.605
1.226
1, 3
2', 4', 6',
8', 9', 10'
3', 5', 7'
0.48
2.11
1.00
3H
12H
6H
10000
5000
0
2.00
1.50
ppm (f1)

^{13}C NMR Spectra

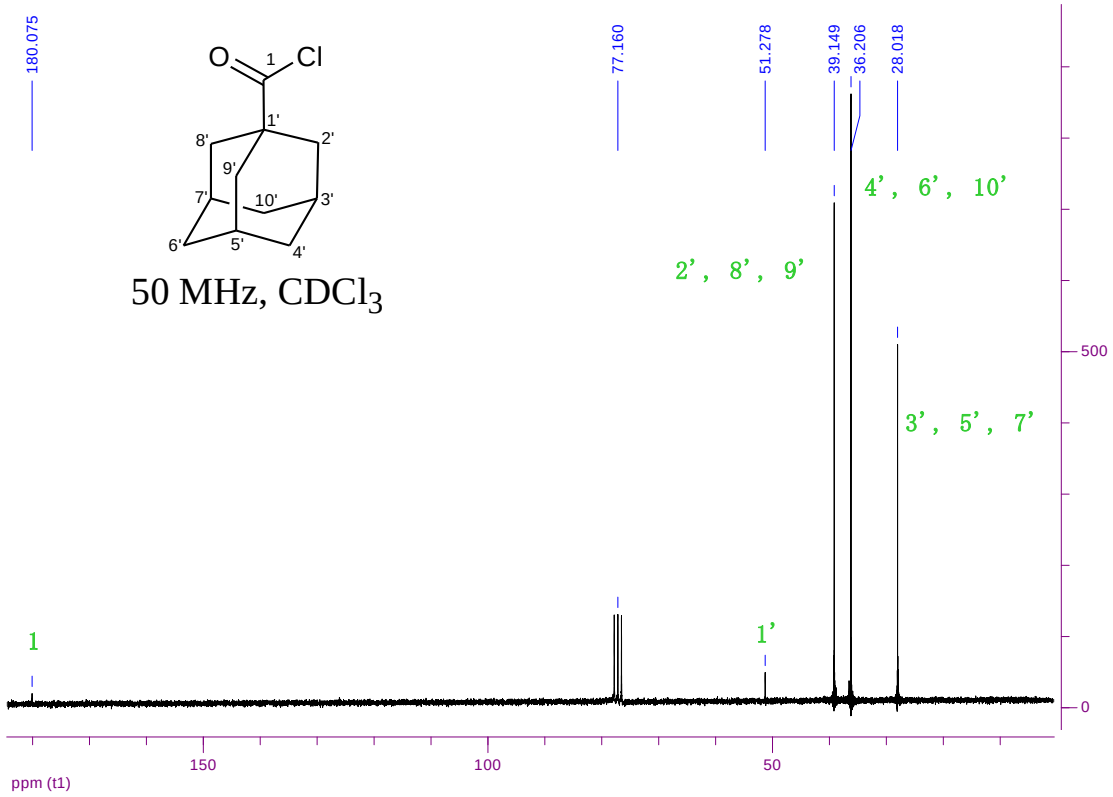

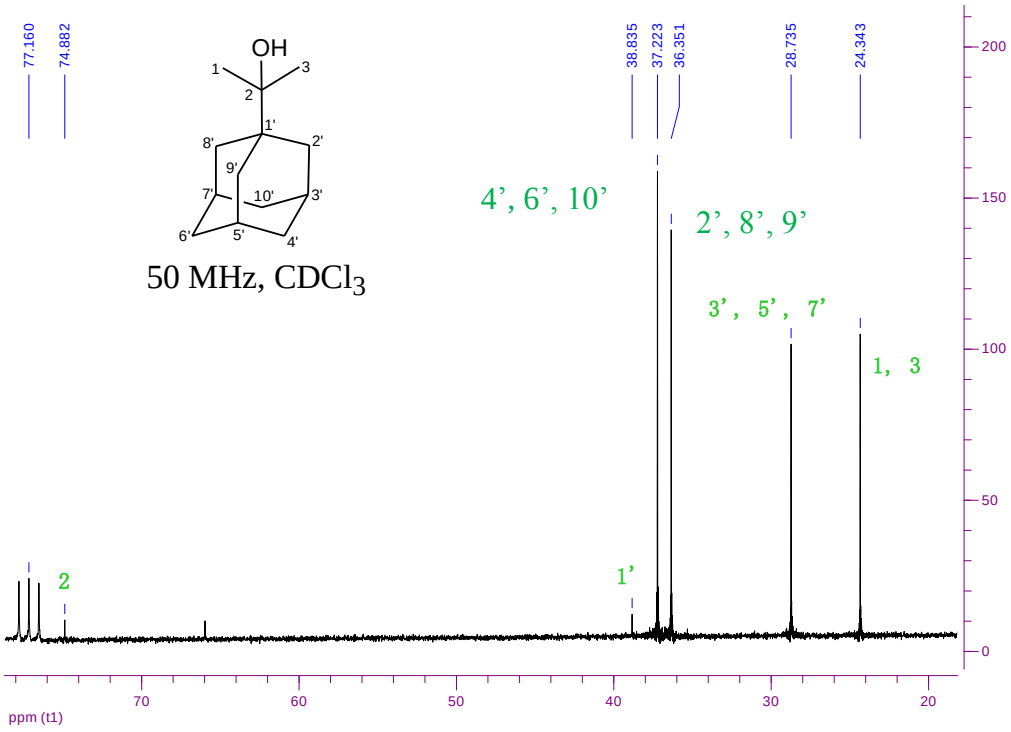
77.160
74.882
OH
38.835
37.223
36.351
28.735
24.343
4', 6', 10'
2', 8', 9'
3', 5', 7'
1, 3
2
1'
50 MHz, CDCl3
ppm (t1)

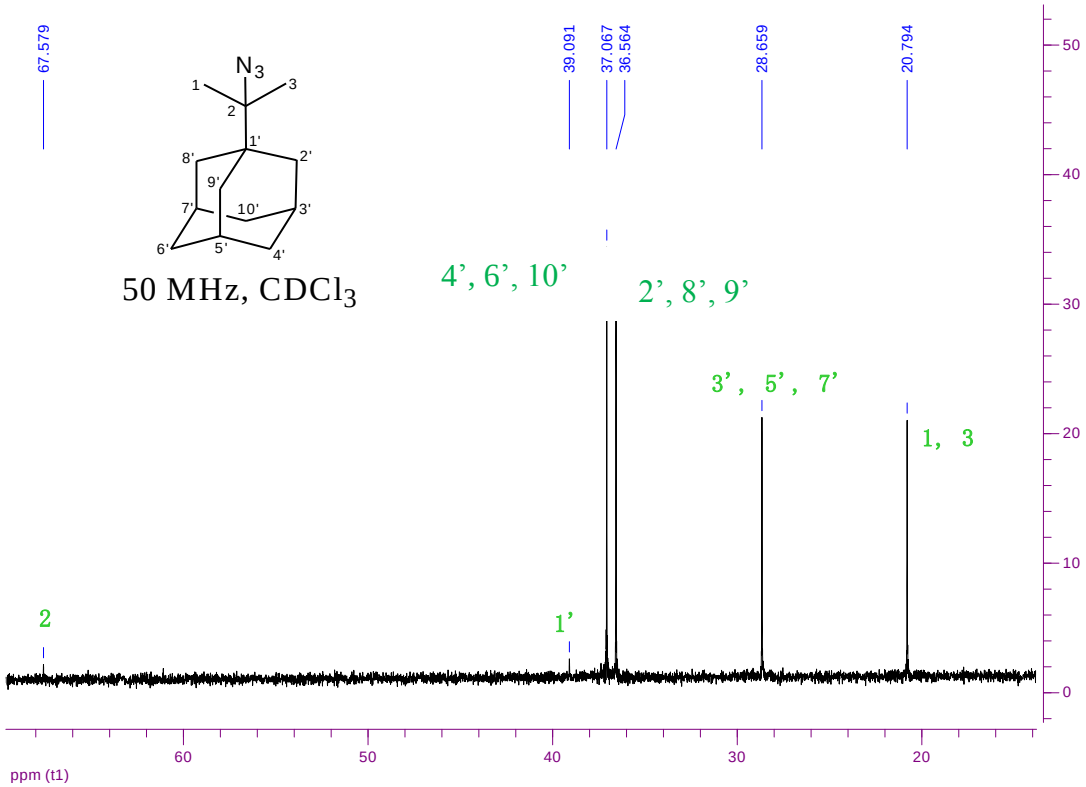
67.579
N3
39.091
37.067
36.564
28.659
20.794
4', 6', 10'
2', 8', 9'
3', 5', 7'
1, 3
2
1'
50 MHz, CDCl3
ppm (t1)

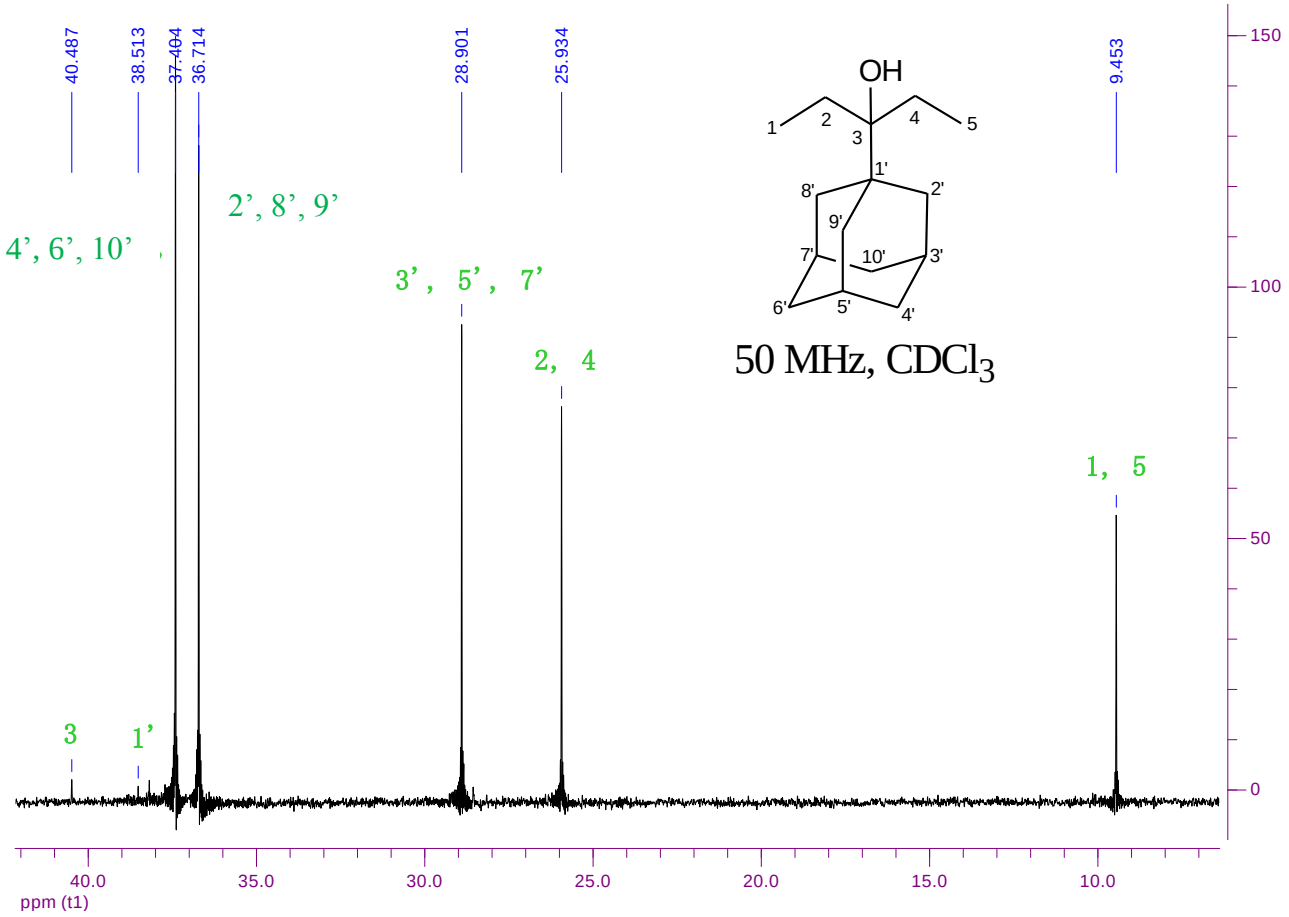
40.487
38.513
37.404
36.714
28.901
25.934
9.453
4', 6', 10'
2', 8', 9'
3', 5', 7'
2, 4
1, 5
3
1'
OH
50 MHz, CDCl3
150
100
50
0
40.0
35.0
30.0
25.0
20.0
15.0
10.0
ppm (t1)

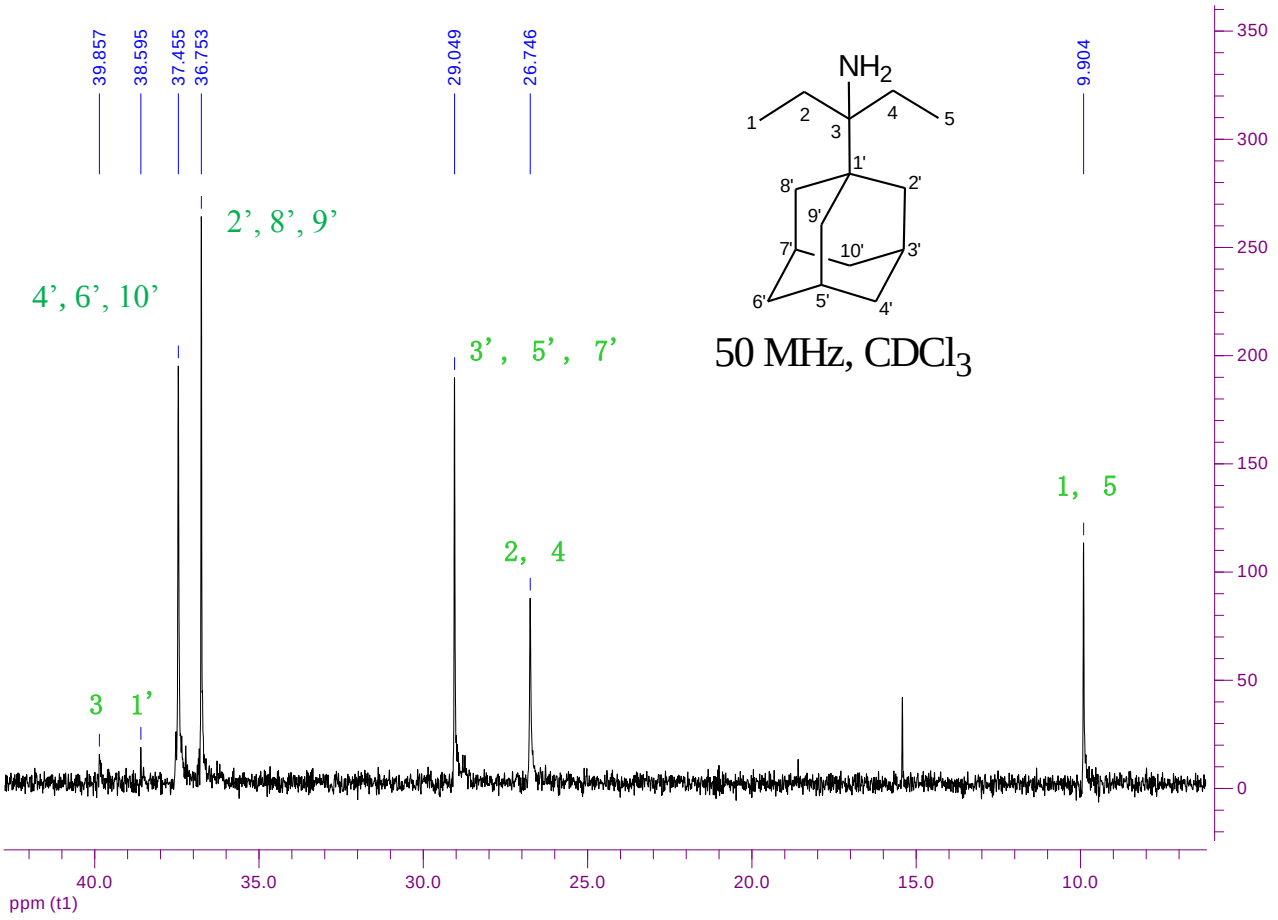
39.857
38.595
37.455
36.753
29.049
26.746
9.904
NH2
1
2
3
4
5
1'
2'
3'
4'
5'
6'
7'
8'
9'
10'
2', 8', 9'
4', 6', 10'
3', 5', 7'
1, 5
2, 4
3
1'
50 MHz, CDCl3
350
300
250
200
150
100
50
0
40.0
35.0
30.0
25.0
20.0
15.0
10.0
ppm (t1)

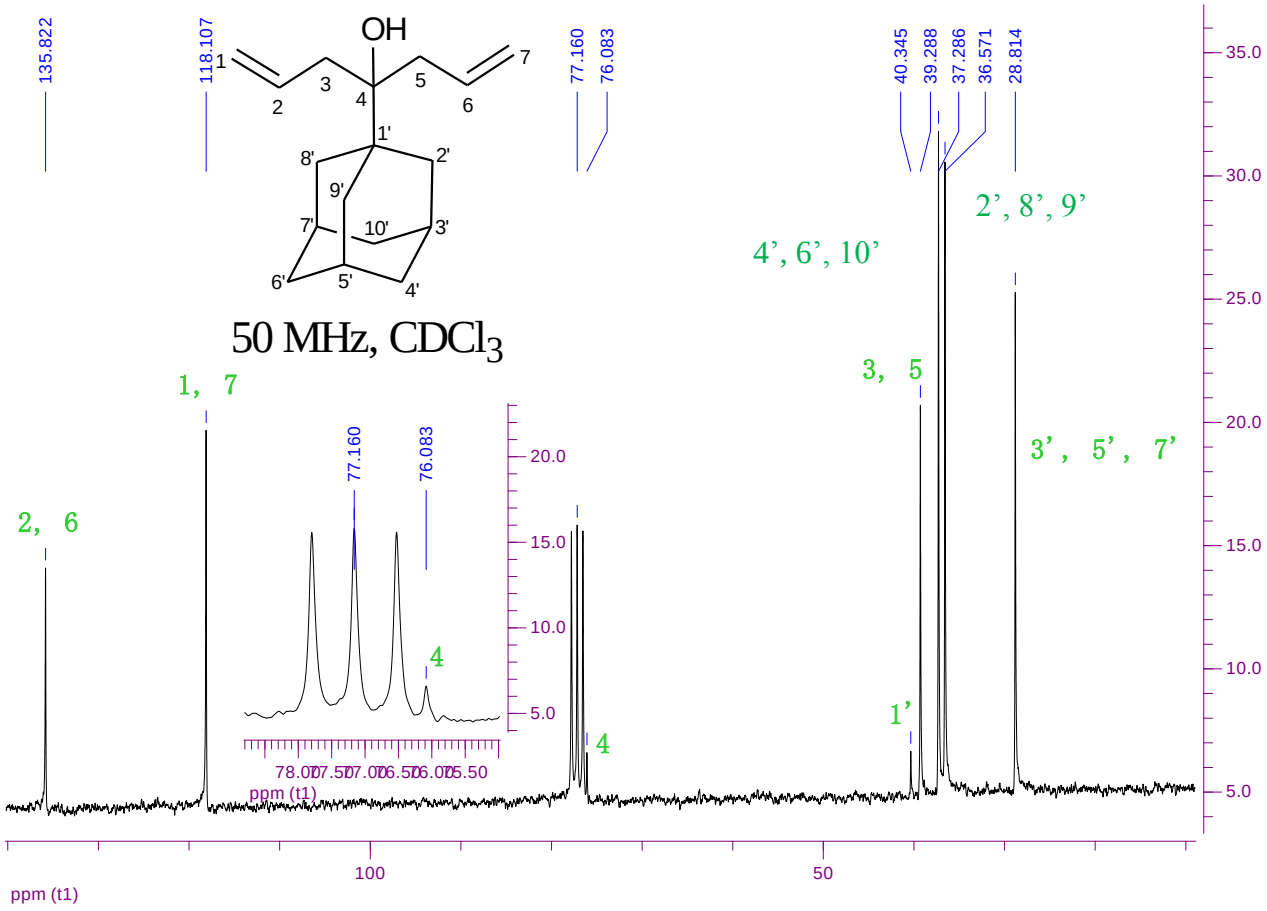
135.822
118.107
OH
1
2
3
4
5
6
7
1'
2'
3'
4'
5'
6'
7'
8'
9'
10'
77.160
76.083
40.345
39.288
37.286
36.571
28.814
50 MHz, CDCl3
1, 7
2, 6
3, 5
4
4
1'
2', 8', 9'
4', 6', 10'
3', 5', 7'
ppm (t1)
100
50
35.0
30.0
25.0
20.0
15.0
10.0
5.0

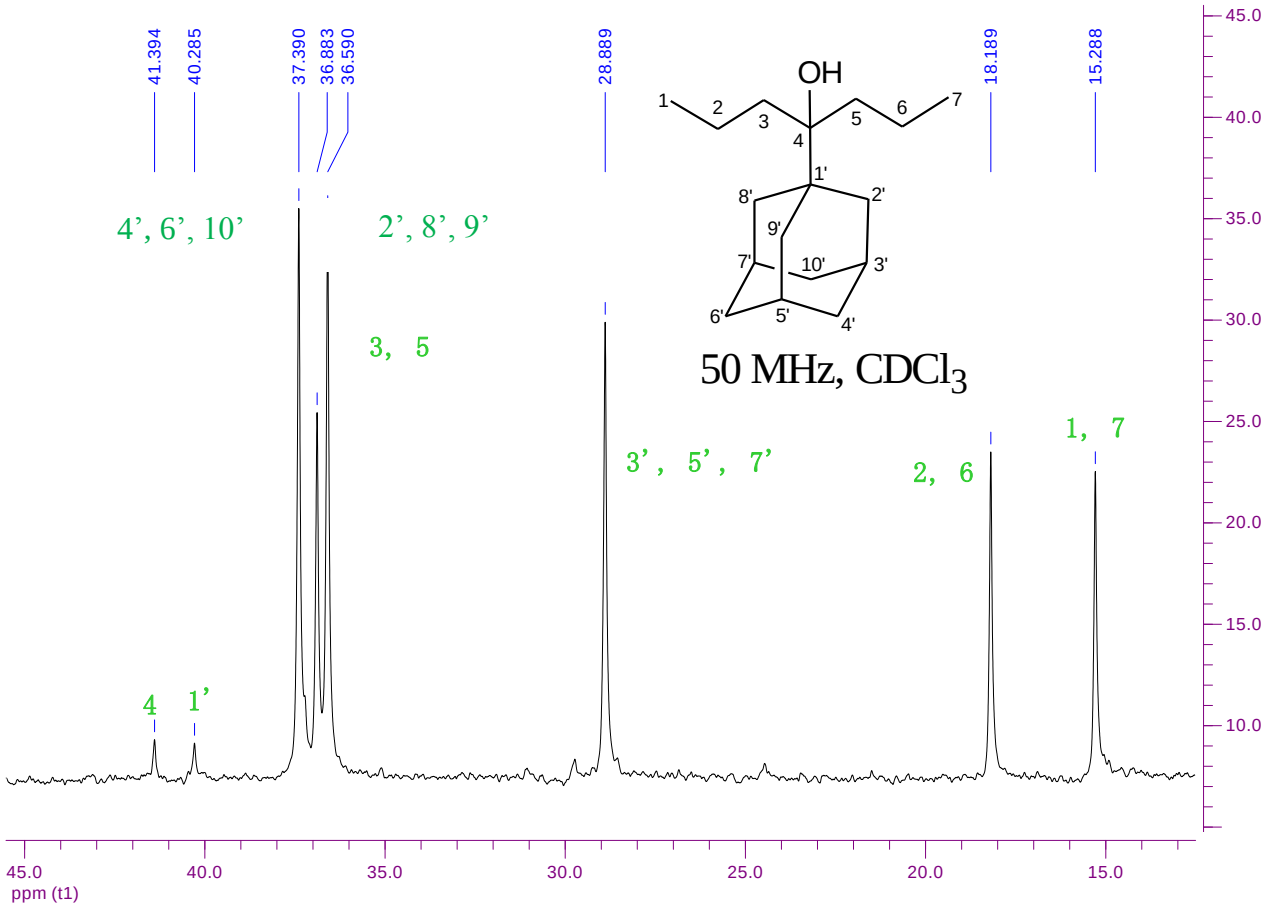
41.394
40.285
37.390
36.883
36.590
28.889
18.189
15.288
4', 6', 10'
2', 8', 9'
3, 5
3', 5', 7'
2, 6
1, 7
4
1'
OH
50 MHz, CDCl3
45.0
40.0
35.0
30.0
25.0
20.0
15.0
10.0
ppm (t1)

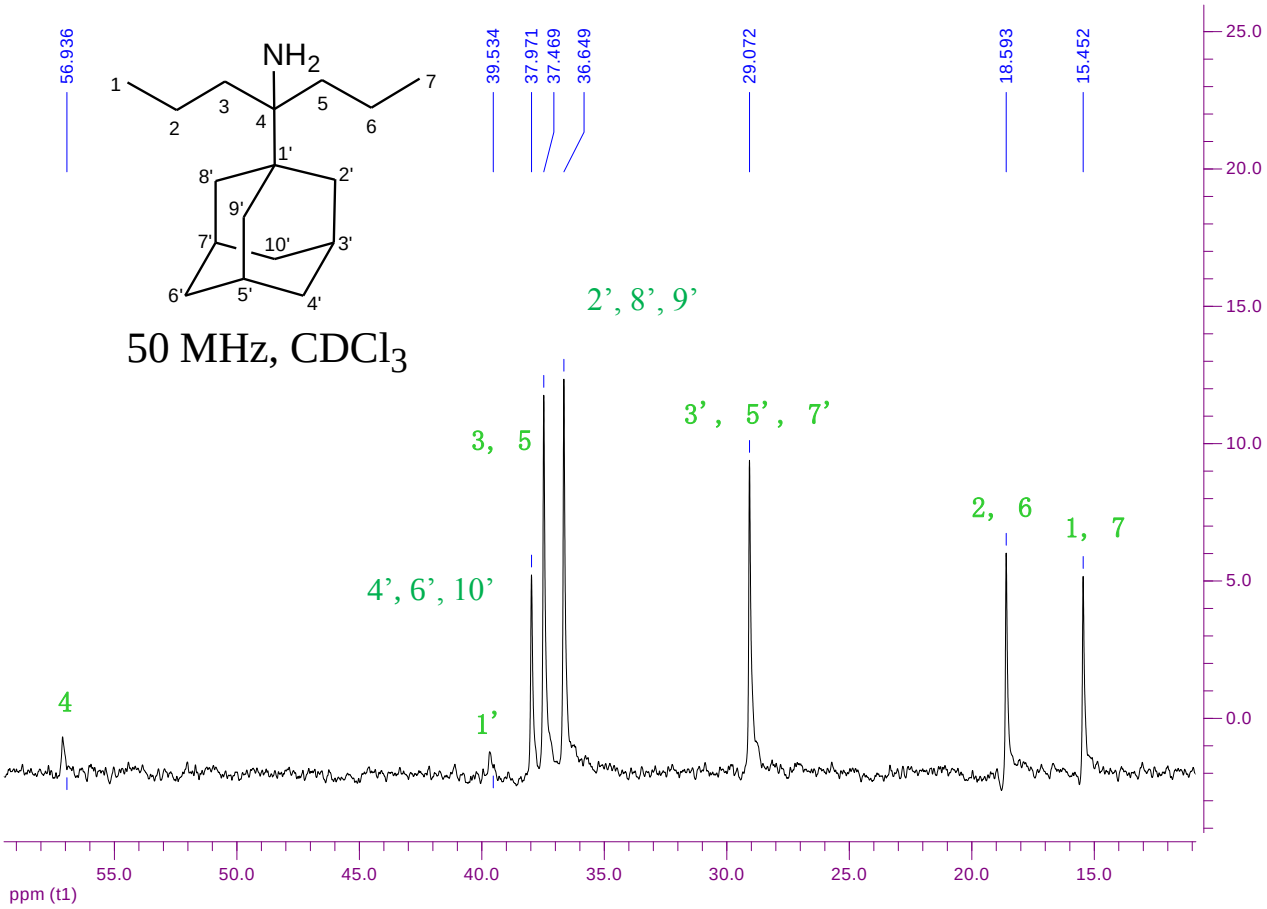
56.936
39.534
37.971
37.469
36.649
29.072
18.593
15.452
NH2
1
2
3
4
5
6
7
1'
2'
3'
4'
5'
6'
7'
8'
9'
10'
50 MHz, CDCl3
2', 8', 9'
3', 5', 7'
3, 5
2, 6
1, 7
4', 6', 10'
4
1'
25.0
20.0
15.0
10.0
5.0
0.0
55.0
50.0
45.0
40.0
35.0
30.0
25.0
20.0
15.0
ppm (t1)

ITC measurements

Binding affinities of aminoadamantane derivatives (see Scheme 1 in the main text) for A/Udorn/72 M2TM were determined by ITC experiments for M2TM-ligand systems in DPC micelles at pH 8. All measurements were performed in triplicate with a TAM 2277 (TA Instruments) at pH 8 and 20 °C in a buffer of 50 mM NaH_2PO_4 and 100 mM NaCl. The peptide and the aminoadamantane derivative were dissolved in a freshly prepared DPC solution with a concentration of 13 mM. Measurements were conducted using 2 mL of 125 µM peptide (corresponding to 31.25 µM M2TM tetramer). A ligand concentration of 1.1 mM was used for the titrant, of which 7.6 µL (equivalent to 8.4 nmol) were dispensed in the peptide/DPC solution with each injection. The time interval between two injections was set to at least 6 minutes, allowing sufficient time for relaxation of the equilibrium.

Synthetic M2TM (residues 22-46) was reconstituted at a 1:57 monomer/lipid ratio - which guarantees the quantitative formation of M2TM tetramers (see ref. 40, 41 of the draft) - in DPC micelles at pH 8 by dissolving and sonicating 225 nmol of M2TM with the 57-fold higher amount of DPC in the aforementioned buffer system. Solutions of ligands **1**, **2**-*R*, **2**-*S*, and **3**-**5** in the buffer were titrated into the calorimetric cell at 20°C. The heat evolved was obtained from the integral of the calorimetric signal. The heat associated with the binding of the ligand to M2TM was obtained by subtracting the heat of dilution from the heat of reaction. [3,4] Data evaluation was carried out with Digitam for Windows v4.1.

Affinity constants were calculated by non-linear regression of the measured heat per injection using Origin 8.0 [5] and are included in Table 1. For the calculation, the concentration of the peptide was kept variable because the M2TM tetramer formation is not complete. Data of three independent measurements was used, whereby all measurements were performed with the same experimental conditions using one stock solution. Data evaluation was done by plotting the measured heat per amount of substance against the molar ratio of titrant to peptide tetramer. The resulting titration curve was fitted using a global fit including the data of the three independent measurements.

ITC is a widely used method in drug discovery, especially in quantitative structure-activity-relationship studies. [6-8] However, there are some inherent limitations with respect to the overall applicability of this method. Since warmth released or consumed by an interaction is detected, the bigger the change of enthalpy during an interaction, the easier this interaction can be measured with ITC. A further limitation is set by the affinity of the interaction. The product of dissociation constant and receptor concentration (called Wiseman constant) determines the slope of the resulting titration curve and should be optimally between 10 and 100. [6-8] For very high affinity interactions, one needs to dilute the system. For low affinity interactions (i.e., K_d values in the range of 10 µM) a very high quantity of the receptor is needed, and this is accompanied with difficulties due to limitations such as availability, cost, solubility, or stability. For the M2TM peptide investigated in this study, the solubility in the DPC micelles limits the possible concentration. Consequently, affinity constants of low affinity binders e.g. **5** against M2TM S31N possess relatively large errors.

Supplementary Tables

Table 1 legend.

[1] See Scheme 1. [2] Binding constant K_d in µM calculated from measured K_a in M^{-1} by $K_d = 1/K_a \times 10^{-6}$ and error in K_d in µM determined by $K_{d,\,error} = (K_{a,\,error}/K_a^2) \times 10^{-6}$. [3] In kcal mol^{-1}. [4] Free energy of binding computed from K_d by $\Delta G = -RT \ln(K_d^{ref}/K_d)$ with K_d^{ref} = 1 M and T = 300 K and error in ΔG determined according to $\Delta G_{error} = \sqrt{\left(\frac{R\,T\,K_{d,error}}{K_d}\right)^2}$ with T = 300 K. [5] Enthalpy of binding and error in the enthalpy calculated from measured binding enthalpy and measured error by $\Delta H = \Delta H_{measured}$ (T / $T_{measured}$) with T = 300 K and the temperature at which the ITC measurements were performed $T_{measured}$ = 293.15 K. [6] Entropy of binding calculated by $\Delta S = (-\Delta G + \Delta H)/T$ and error in ΔS computed by the equation $\Delta S_{error} = \sqrt{\Delta G_{error}^{\ 2} + \Delta H_{error}^{\ 2}}$ [7] No detectable binding. [8] Values could not be determined reliably due to the limitations of the methods in the area of very weak binding.

Table S1. Block [1] of full-length Udorn M2 V28I-dependent current [2] by selected compounds.

Compound	Udorn M2 V28I			
	% Block after 2 min	% Block after 5 min	IC_{50} after 2 min (µM)	IC_{50} after 5 min (µM)
1	66.5 ± 1.4%	88.8 ± 1.4%	ND [3]	ND [3]
2	84 ± 1%	93 ± 0%	ND [3]	ND [3]
2-*R*	71 ± 1%	90 ± 1%	ND [3]	ND [3]
2-*S*	78 ± 1%	92 ± 0%	ND [3]	ND [3]
3	56 ± 3%	80 ± 2%	52.0	17.9
4	43 ± 2%	72 ± 2%	124.5	53.8
5	ND [3]	ND [3]	ND [3]	ND [3]

[1] For each compound, percent block of pH-dependent M2 current at listed concentrations (+/- s.e.m.) and IC_{50} (µM) is shown. [2] Three or four (for compound **2**-*S*) or two (for **1**) replicates were used for measurements at 100 µM. [3] ND: Not determined.

Table S2. Structural and dynamic measures from MD trajectories of A/Udorn/72 M2TM-ligand complexes in DMPC bilayer (4 ns).[7]

Ligand [1]	RMSD (Cα) [2]	Angle C-N vector [3]	V27-Ad [4]	H-bonds [5]	Cl-N distance [6]
1 [2]	1.5 ± 0.1	11.2 ± 5.9	4.2 ± 0.3	2.7 ± 0.5	32.3 ± 6.6
2-*R*	1.5 ± 0.2	44.7 ± 7.6	3.9 ± 0.273	2.6 ± 0.6	33.3 ± 5.8
2-*S*	1.1 ± 0.2	55.7 ± 6.1	4.2 ± 0.259	2.8 ± 0.4	35.9 ± 5.9
3	1.4 ± 0.2	51.5 ± 4.9	4.4 ± 0.3	2.9 ± 0.3	33.7 ± 6.3
4	1.0 ± 0.1	47.5 ± 6.9	4.5 ± 0.3	2.9 ± 0.3	35.7 ± 7.5
5	1.5 ± 0.2	49.4 ± 4.3	4.4 ± 0.2	2.9 ± 0.3	30.0 ± 6.0

Table S3. Structural and dynamic measures from MD trajectories of A/Udorn/72 M2TM-ligand complexes in DMPC bilayer (80 ns).[7]

Ligand [1]	RMSD (Cα) [2]	Angle C-N vector [3]	V27-Ad [4]	H-bonds [5]	Cl-N distance [6]
1 [2]	1.2 ± 0.2	9.8 ± 5.4	4.2 ± 0.3	2.7 ±0.5	23.5 ± 9.3
2-*R*	1.8 ± 0.5	52.0 ± 6.7	4.2 ± 0.3	2.6 ± 0.5	34.2 ± 6.5
2-*S*	1.2 ± 0.2	50.9 ± 5.3	4.1 ± 0.3	2.9 ± 0.3	33.7 ± 7.4
3	1.2 ± 0.2	53.8 ± 8.3	4.1 ± 0.2	2.9 ± 0.3	32.7 ± 6.1
4	1.6 ± 0.5	54.3 ± 6.9	4.4 ± 0.3	2.9 ± 0.3	33.9 ± 7.7
5	1.0 ± 0.2	61.5 ± 7.1	4.5 ± 0.4	2.9 ± 0.3	32.4 ± 7.4

[1] See Scheme 1; measures for **1** were added for comparison reasons.
[2] Maximum root-mean-square deviation (RMSD) for Cα atoms of M2TM relative to the initial structure (PDB entry: 2KQT) after root-mean-square fitting of Cα atoms of M2TM; in Å.
[3] Angle between the vector along the bond from the carbon atom of the adamantane core to the ligand nitrogen atom and the normal to the membrane; in degrees.
[4] Mean distance between center of mass of V27 and centers of mass of adamantane calculated using Gromacs tools; in Å.
[5] Mean number of H-bonds between ligand's ammonium group and waters.
[6] Mean distance in Å between the ligand N and the nearest Cl^-.
[7] The axial position of the six compounds 1, 2, 2-*R*, 2-*S*, and 3-5 inside the pore differed only slightly, that is, 0-0.3 Å towards the C-end, relative to 1. The simulated M2TM-ligand complexes were stable, and in all cases the M2TM tetramer showed no large conformational changes in the course of the simulations, as demonstrated by RMSDs ≤ 1.8 Å for M2TM Cα-carbons with respect to the initial structure.

Table S4. Structural and dynamic measures from MD trajectories of M2TM S31N-ligand complexes in DMPC bilayer (80 ns).

Ligand [1]	RMSD (Cα) [2]	Angle C-N vector [3]	V27-Ad [4]	H-bonds with waters [5]	H-bonds with N31-CO [6]	Cl-N distance [7]
1	2.6 ± 0.4	112.3±27	5.2 ± 0.7	1.4 ± 0.7	1.2 ± 0.9	34.3 ± 7.9
3	1.8 ± 0.3	122.3±8.7	6.9 ± 0.1	1.9 ± 0.7	1.0 ± 0.7	34.3 ± 7.9
5	1.8 ± 0.3	115.1±5.2	6.3 ± 0.4	1.7 ± 0.8	1.1 ± 0.8	33.4 ± 7.1

[1] See Scheme 1; values taken from ref. 27 of the draft; measures for **1** were added for comparison reasons.
[2] Maximum root-mean-square deviation (RMSD) for Ca atoms of M2TM relative to the initial structure (PDB entry: 2KQT) after root-mean-square fitting of Ca atoms of M2TM; in Å.
[3] Angle between the vector along the bond from the carbon atom of the adamantane core to the ligand nitrogen atom and the normal of the membrane; in degree.
[4] Mean distance between center of mass of V27 and centers of mass of adamantane calculated using Gromacs tools; in Å.
[5] Mean number of H-bonds between ligand's ammonium group and waters.
[6] Mean number of H-bonds between a ligand's ammonium group and N31 carbonyl group.
[7] Mean distance in Å between the ligand N and the nearest Cl^-.

Table S5. Area per lipid for values from MD simulations of Amt-M2TM complex and experimental values.

Lipid	Average Area per lipid (Å^2)	Number of lipids	Min value (Å^2)	Max value (Å^2)	Ensemble	Experiment
DMPC	61.84	47	59.61	63.64	NPT	60.6±0.5

Supplementary Figures

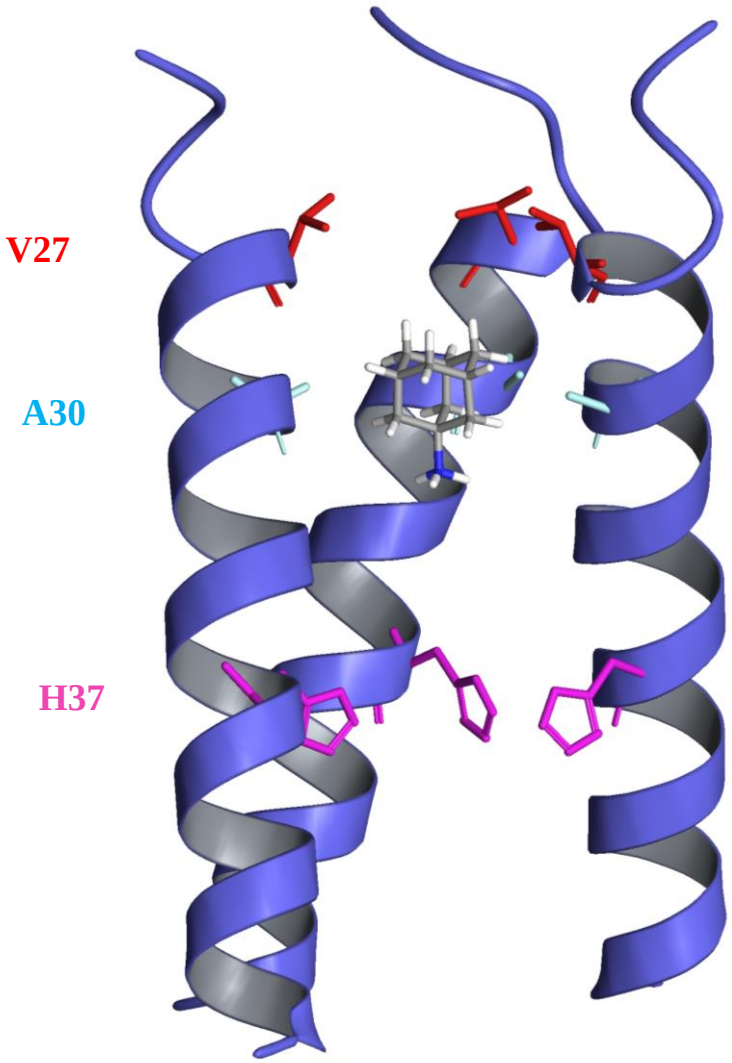

Figure S1. Structure and amino acid sequence of M2TM WT. Cartoon representation of M2TM (PDB entry: 2KQT) with critical residues for binding: V27 (red), A30 (light blue), His37 (pink) depicted as sticks. Side view of M2TM; one monomer of the tetramer was removed for visualization purposes; the N-terminal end is at the top. The amino acid sequence of M2TM WT corresponding to 2KQT: SSDPLVVAASIIGILHLILWILDRL.

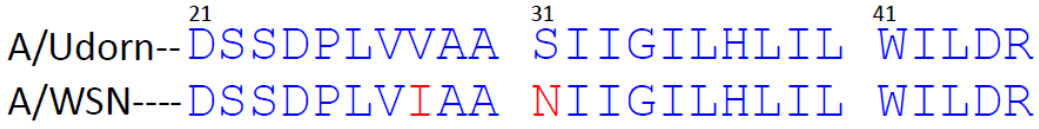

Figure S2. Transmembrane domain sequence for A/Udorn/72 (and A/Hong Kong/68) compared to A/WSN/33, which differ at positions 28 and 31.

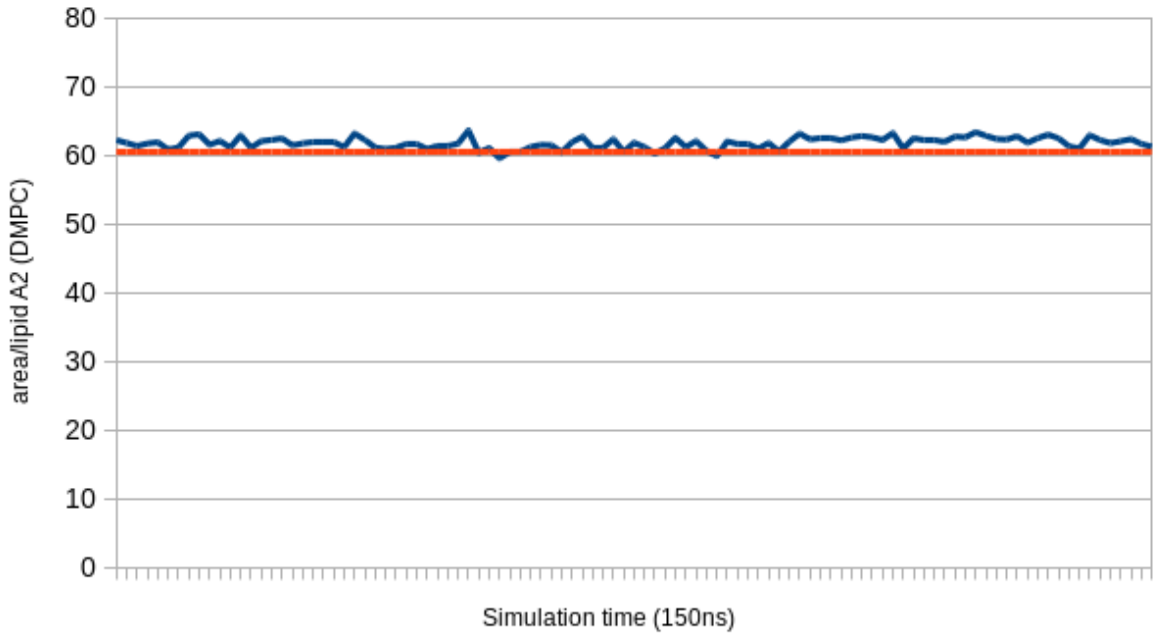

Figure S3. Time courses of the average area per lipid for Amt-M2TM complex in DMPC; red line is the experimental value of the area per lipid DMPC for the pure bilayer (60.6 $Å^2$).

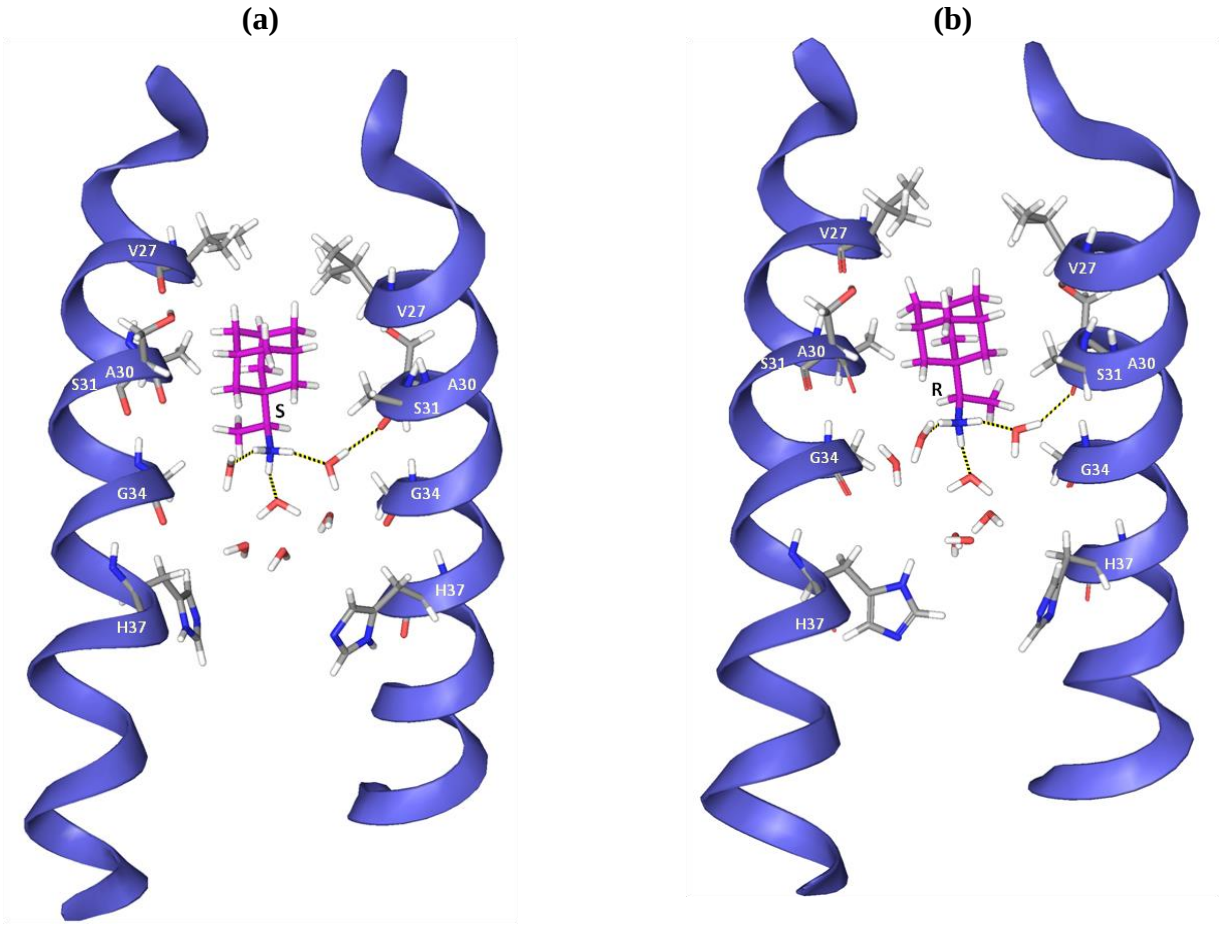

Figure S4. Representative snapshots from the simulation of ligands **2**-*R* (a), **2**-*S* (b) bound to M2TM WT. Six and seven water molecules are shown between the ligand and H37 residues for **2**-*S* and **2**-*R* respectively. Three hydrogen bonds between the ammonium group of the ligand and three water molecules are shown. Hydrogen bonding with water molecules and van der Waals interactions of the adamantane core with V27 and A30 side chains stabilize the ligand inside the pore with its ammonium group oriented towards the C-terminus of the channel. The $CHCH_3$ group that includes the chiral carbon in **2**-*R* and **2**-*S* is positioned in the cleft between G34 and A30. A30 has different van der Waals interactions between the two enantiomers, being a chiral amino acid. However, the distance between the ligand CH_3 and the A30 CH_3 is similar for the two enantiomers (3.9 ± 0.3 and 3.5 ± 0.3 Å respectively); also the distance between V27-Ad (4.2 ± 0.3 and 4.1 ± 0.3 Å respectively see Table S3).

Supplementary References

1. Hansen, R. K.; Broadhurst, R. W.; Skelton, P. C.; Arkin, I. T. Hydrogen/deuterium exchange of hydrophobic peptides in model membranes by electrospray ionization mass spectrometry. *Journal of the American Society for Mass Spectrometry* **2002**, *13*, 1376-87.
2. Kolocouris, A.; Zikos, C.; Broadhurst, R. W. ^{19}F NMR detection of the complex between amantadine and the receptor portion of the influenza A M2 ion channel in DPC micelles. *Bioorg. Med. Chem. Letters* **2007**, *17*, 3947–3952.
3. Wiseman, T.; Williston, S.; Brandts, J. F.; Lin, L. N. Rapid measurement of binding constants and heats of binding using a new titration calorimeter. *Analytical biochemistry* **1989**, *179*, 131-137.
4. Doyle, M. L. Characterization of binding interactions by isothermal titration calorimetry. *Current opinion in biotechnology* **1997**, *8*, 31-35.
5. *Origin 8.1G SR1*, v8.1.13.88; OriginLab Corporation, Northampton, MA, USA: **2009**.
6. Ladbury, J. E.; Klebe, G.; Freire, E. Adding calorimetric data to decision making in lead discovery: a hot tip. *Nat. Rev. Drug Discov.* **2010**, *9*, 23-27.
7. Chaires, J. B. Calorimetry and thermodynamics in drug design. *Annu. Rev. Biophys.* **2008**, *37*, 135-151.
8. Perozzo, R.; Folkers, G.; Scapozza, L. Thermodynamics of protein-ligand interactions: history, presence, and future aspects. *J. Recept. Signal Transduct. Res.* **2004**, *24*, 1-52.